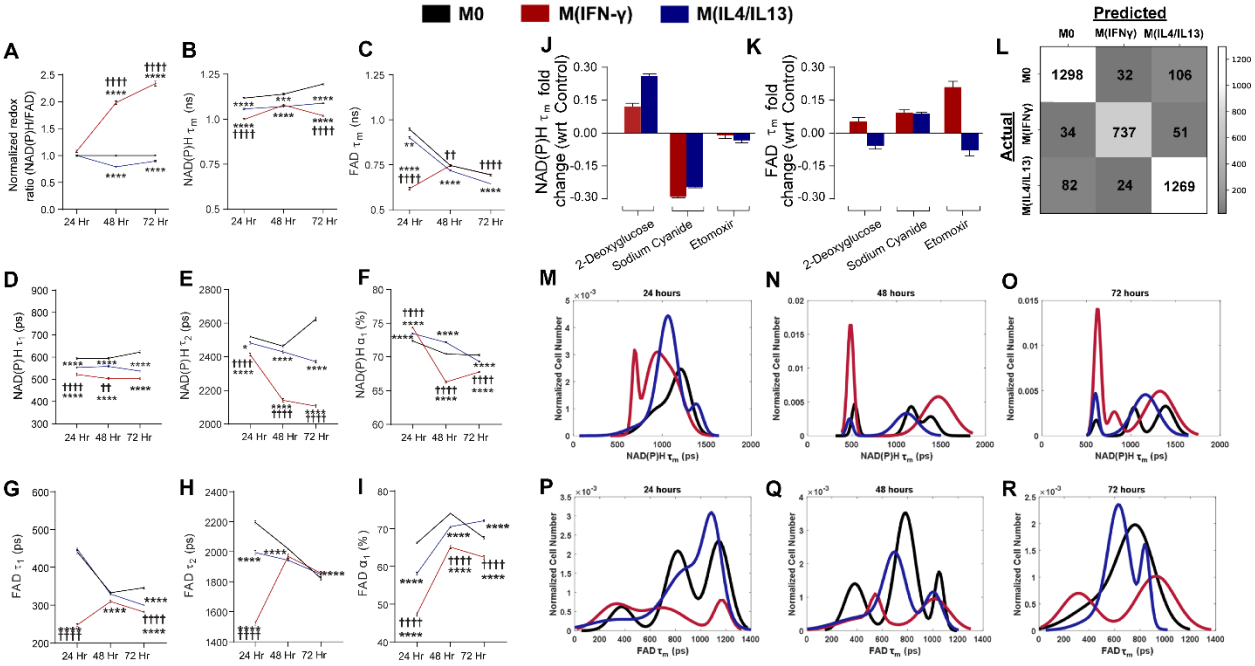

Supplementary Figure 1: Fluorescence lifetimes of NAD(P)H and FAD exhibit differences between macrophage polarization states. Quantitative measurement of A) Redox Ratio, B) NAD(P)H τ_m, C) FAD τ_m, D) NAD(P)H τ_1, E) NAD(P)H τ_2, F) NAD(P)H α_1, G) FAD τ_1, H) FAD τ_2, I) FAD α_1, illustrate metabolic differences across 2D cultures of RAW264.7 macrophages polarized to M0, M(IFN-γ), and M(IL4/IL13) over a 72-hour timecourse. (**, ***, ****p<0.01,0.001, 0.0001 vs. M0; ††, †††† p<0.01,0.0001 vs. M(IL4/IL13)) Fold change of J) NAD(P)H τ_m and K) FAD τ_m in response to treatment with 2-deoxyglucose, sodium cyanide, and etomoxir in M(IFN-γ) and M(IL4/IL13) macrophages shows metabolic inhibitor treatment alters NAD(P)H and FAD mean lifetimes of 2D polarized mouse macrophages. L) Graphical representation of confusion matrix for random forest classification of M0, M(IFNγ), and M(IL4/IL13) RAW264.7 mouse macrophages at all time points. Values along the diagonal (upper left to lower right) represent number of correctly classified cells per condition, while all other row values represent the number of misclassified cells for the respective condition. Population distribution modeling demonstrates metabolic heterogeneity for single-cell NAD(P)H τ_m over M) 24 hours, N) 48 hours, and O) 72 hours and FAD τ_m over P) 24 hours, Q) 48 hours, and R) 72 hours in macrophages unstimulated (M0) and stimulated to M(IFN-γ) and M(IL4/IL13).

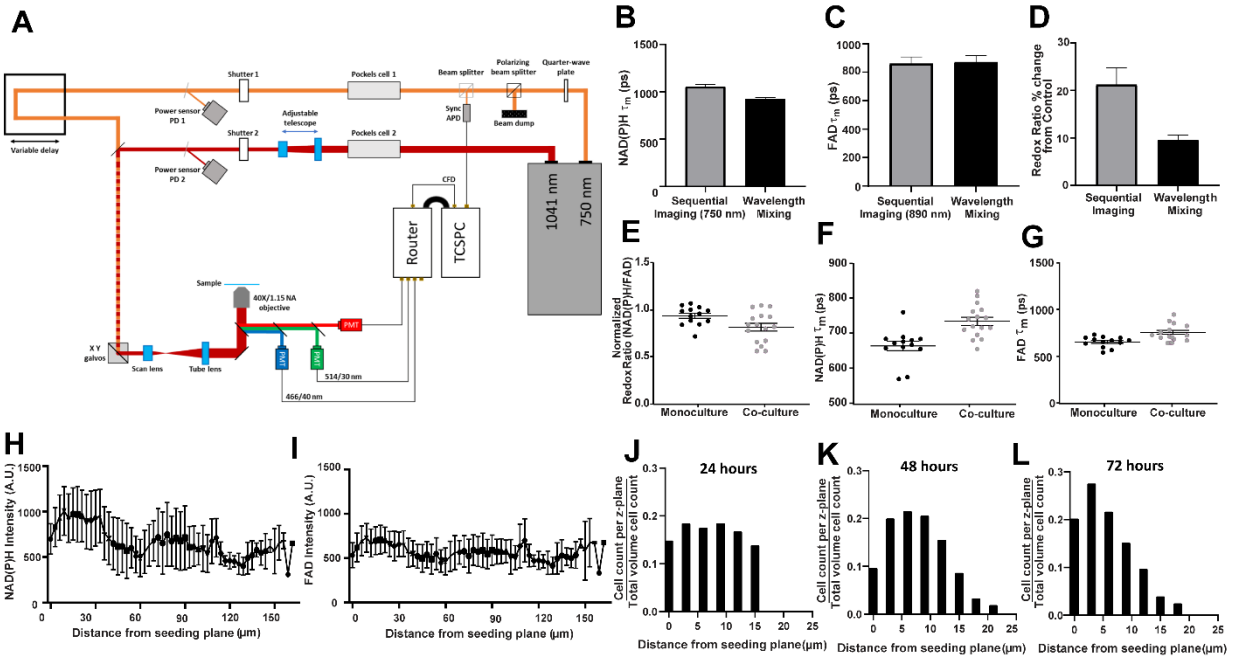

Supplementary Figure 2: Validation of two-photon wavelength mixing for evaluating autofluorescence and migration effects in 2D cultures and the 3D Stacks microfluidic platform A) Diagram of wavelength mixing two-photon system (APD – avalanche photodiode, CFD – constant fraction discriminator, PD – photodiode, PMT – photomultiplier tube, TCSPC – time-correlated single photon counting electronics). Metabolic autofluorescence measurements were first assessed for consistency between sequential, two-color imaging and wavelength mixing approaches. Comparison of absolute values of B) NAD(P)H τ_m, and C) FAD τ_m in BT474 cells imaged with two-color imaging and wavelength mixing demonstrates similar fluorescence decay rate of both fluorophores. D) Relative fold change of Redox Ratio between control and sodium cyanide-treated BT474 human breast carcinoma cells imaged with the sequential, two-color imaging and wavelength mixing. Trends in redox measurements are conserved between both imaging techniques. Non-specific metabolic changes were evaluated from quantitative measurement of E) redox ratio, F) NAD(P)H τ_m, and G) FAD τ_m across 3D RAW264.7 macrophage monocultures or co-cultures of Polyoma Middle T-virus (PyVMT) breast cancer and RAW264.7 macrophages 1 hour post-seeding. Significant differences were not observed in redox or lifetime measurements between monocultured and co-cultured macrophages, demonstrating metabolic autofluorescence of monoculture and co-cultured macrophages are similar upon initial seeding. Additionally, single-cell measurements for H) NAD(P)H and I) FAD autofluorescence intensity with respect to distance from the macrophage seeding plane demonstrate no appreciable depth-dependent attenuation in collagen I ECM microwells imaged over 170 μm depths. RAW264.7 macrophages were seeded at the top and bottom of 3D ECM layers, and migration was measured at J) 24 hours, K) 48 hours, and L) 72 hours. Migration was quantified from cell counts at each 3 μm slice divided by the total cell count across the entire 3D macrophage layer. RAW264.7+RAW264.7 co-cultures exhibit minimal changes in cell distribution across the collagen layer, suggesting actively-migrating macrophage populations are absent in macrophage-macrophage co-cultures and active migration observed in tumor-macrophage co-cultures is induced by tumor stimuli.

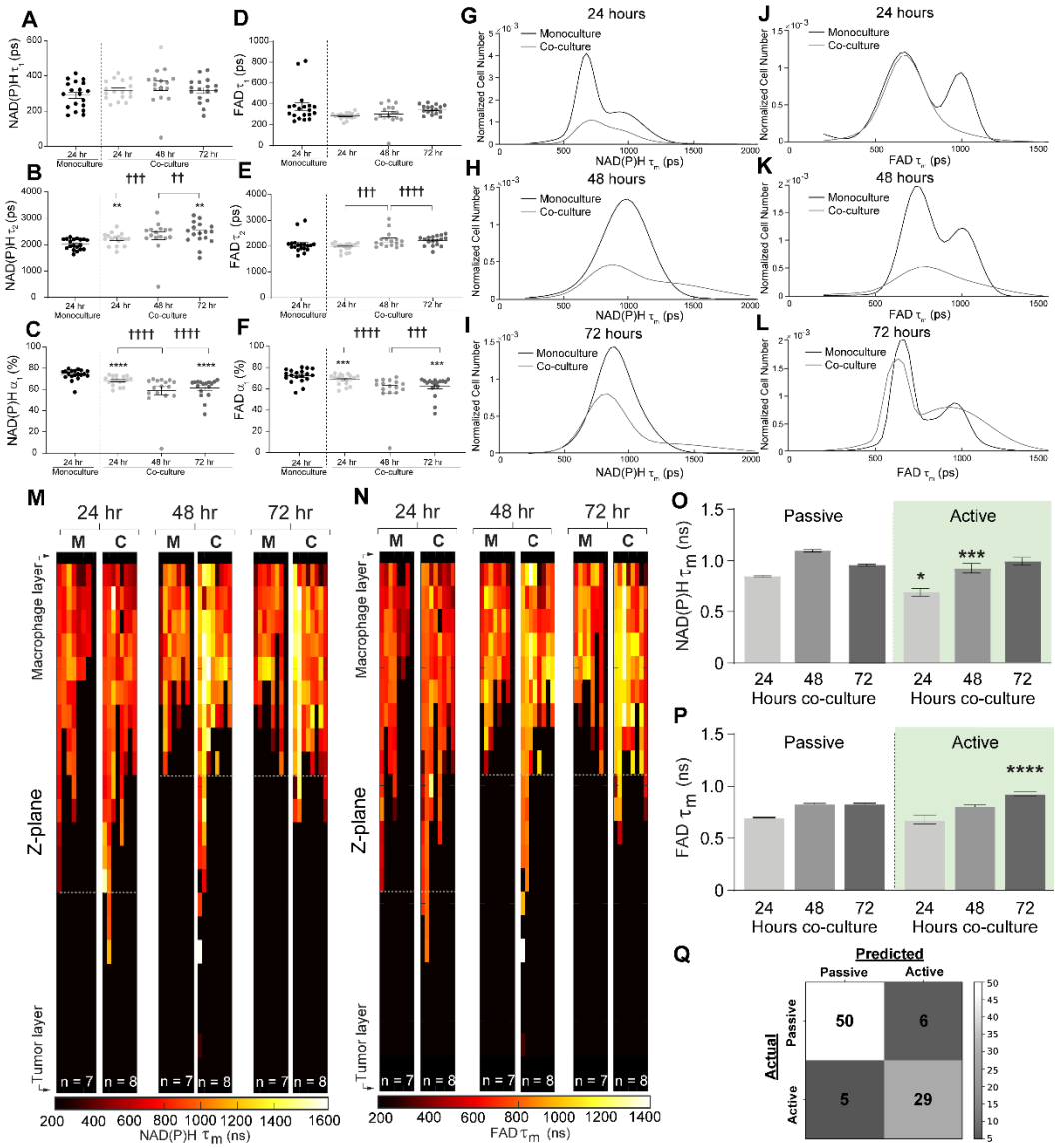

Supplementary Figure 3: Prolonged co-culture of mouse breast cancer and macrophages yields heterogeneous NAD(P)H and FAD fluorescence lifetime and migration compared to monoculture. Quantitative measurement of A) NAD(P)H τ_1, B) NAD(P)H τ_2, C) NAD(P)H α_1, D) FAD τ_1, E) FAD τ_2, F) FAD α_1, across 3D RAW264.7 macrophage monocultures or co-cultures of Polyoma Middle T-virus (PyVMT) breast cancer and RAW264.7 macrophages over 24, 48, and 72 hours. Population distribution modeling of single-cell NAD(P)H τ_m at G) 24 hours, H) 48 hours, and I) 72 hours post-seeding and FAD τ_m at J) 24 hours, K) 48 hours, and L) 72 hours post-seeding in monocultures and co-cultures. Representative heatmaps of M) NAD(P)H τ_m and N) FAD τ_m during RAW264.7 macrophage migration in 3D monocultures and co-cultures with PyVMT breast carcinoma. Both monocultured and co-cultured macrophages display increased heterogeneity in NAD(P)H and FAD lifetime, regardless of time and migration distance. Passively- and actively- migrating macrophage populations were defined in co-cultures over 72 hours to observe time-dependent relationships between O) NAD(P)H τ_m and P) FAD τ_m and migratory activity;*,***,****$p<0.05,0.001,0.0001$ vs passive migration. Q) Graphical representation of confusion matrix for random forest classification of passively- vs. actively-migrating co-cultured RAW264.7 macrophages at all time points, illustrating the number of correctly classified cells per condition.

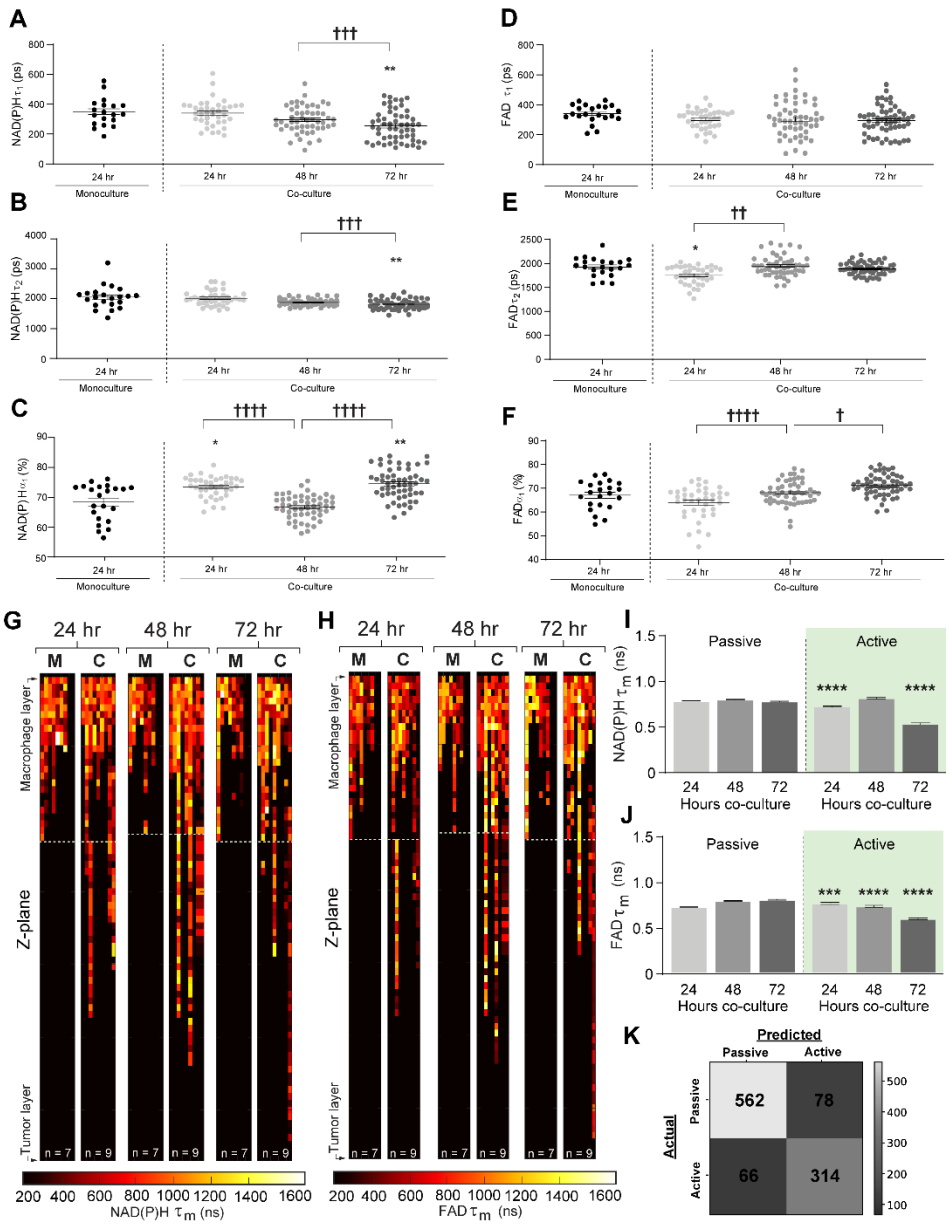

Supplementary Figure 4: Primary human tumor cells stimulate changes in NAD(P)H and FAD fluorescence lifetime and cell migration in co-cultured human monocyte-derived macrophages. Quantitative measurement of A) NAD(P)H τ_1, B) NAD(P)H τ_2, C) NAD(P)H α_1, D) FAD τ_1, E) FAD τ_2, F) FAD α_1 across 3D monocultures of human THP-1s or co-cultures of primary breast cancer cells and THP-1s over 24, 48, and 72 hours. Representative heatmaps of G) NAD(P)H τ_m and H) FAD τ_m during THP-1 migration in 3D monocultures and co-cultures with primary breast carcinoma. Both monocultured monocytes and co-cultured monocyte-derived macrophages exhibit substantial heterogeneity in NAD(P)H and FAD lifetime within z-planes across the 3D layer at all timepoints. Differences in I) NAD(P)H τ_m, and J) FAD τ_m between actively- and passively-migrating populations were quantified at each time point. ***,**** p<0.001,0.0001 vs. passive migration. K) Confusion matrix for random forest classification of passively- vs. actively-migrating co-cultured THP-1 macrophages at all time points.

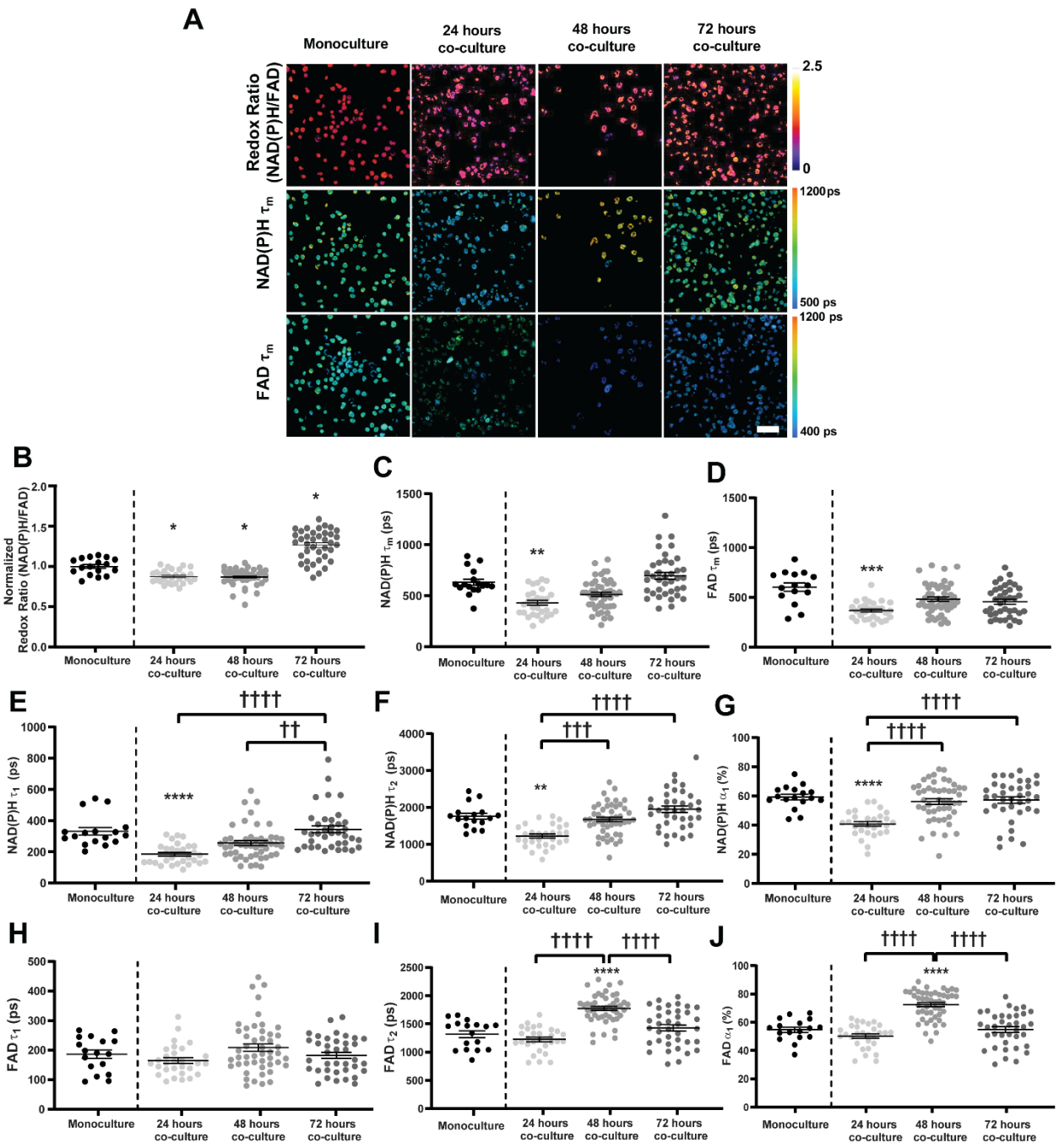

Supplementary Figure 5: Metabolic changes in human THP-1s following co-culture with MDA-MB-231 human breast carcinoma. A) Representative autofluorescence images demonstrate qualitative differences in the optical redox ratio, NAD(P)H τ_m, and FAD τ_m in 3D monocultures of human THP-1s or co-cultures of MDA-MB-231 breast cancer and THP-1s. Scale bar = 50 µm. Quantitative trends in B) redox ratio, C) NAD(P)H τ_m, D) FAD τ_m, E) NAD(P)H τ_1, F) NAD(P)H τ_2, G) NAD(P)H α_1, H) FAD τ_1, I) FAD τ_2, and J) FAD α_1 of monocultures or co-cultures over 24, 48, and 72 hours;*,**,*** $p<0.05,0.01,0.001$ vs monoculture.

Supplementary Table 1: Mouse and Human Macrophage Polarization Gene Panels

Gene Symbol	Refseq #	Official Full Name	Associated Phenotype[38]
Mouse gene panel			
Stat3	NM_011486	signal transducer and activator of transcription 3	M2-like
Vegfa	NM_001025	vascular endothelial growth factor A	M2-like
Ccl5	NM_013653	chemokine (C-C motif) ligand 5	M1-like
Il10	NM_010548	interleukin 10	M2-like
Ptgs2	NM_011198	prostaglandin-endoperoxide synthase 2	M2-like
Ccl2	NM_011333	chemokine (C-C motif) ligand 2	M1-like
Il23a	NM_031252	interleukin 23, alpha subunit p19	M1-like
Ccl22	NM_009137	chemokine (C-C motif) ligand 22	Mixed
Il12b	NM_008352, XM_006532306	interleukin 12b	Mixed
Il1b	NM_008361, XM_006498795	interleukin 1 beta	M1-like
Il6	NM_031168	interleukin 6	Mixed
Nos2	NM_010927, XM_006532446	nitric oxide synthase 2, inducible	Mixed
Cxcl5	NM_009141	chemokine (C-X-C motif) ligand 5	M1-like
Tnf	NM_013693, NM_001278601	tumor necrosis factor	Mixed
Hsp90ab1	NM_008302	heat shock protein 90 alpha (cytosolic), class B member 1	Reference gene
Pgk1	NM_008828	phosphoglycerate kinase 1	Reference gene
Human gene panel			
VEGFA	NM001025366	vascular endothelial growth factor A	M2-like
IL10	NM_000572	interleukin 10	Mixed
PTGS2	NM_000963	prostaglandin-endoperoxide synthase 2	M2-like
CCL2	NM_002982	chemokine (C-C motif) ligand 2	M1-like
CCL22	NM_00990	chemokine (C-C motif) ligand 22	M2-like
IL12B	NM _00187	interleukin 12b	Mixed
IL1B	NM_000576	interleukin 1 beta	M1-like
IL6	NM_000600	interleukin 6	Mixed
NOS2	NM_000625	nitric oxide synthase 2, inducible	Mixed
TNF	NM_000594	tumor necrosis factor	M1-like
CSF1	NM_000757	colony stimulating factor 1 (macrophage)	Mixed
TGFB1	NM_000660	transforming growth factor, beta 1	Mixed
ACTB	NM_001101	actin, beta	Reference gene
B2M	NM_004048	beta-2-microglobulin	Reference gene

Supplementary Table 2: Significance of redox ratio fold change in inhibitor-treated 2D cytokine-stimulated mouse macrophages

Inhibitor	M(IFN-γ)		M(IL4/IL13)	
	Redox ratio fold change relative to M0	p-value	Redox ratio fold change relative to M0	p-value
2-Deoxyglucose	-0.5030	<0.000001	-0.3283	0.000676
Sodium cyanide	0.5729	<0.000001	0.8256	<0.000001
Etomoxir	0.3084	0.000007	0.6204	<0.000001

Supplementary Table 3: Coefficients of variation (CV) and significance of CV equality for optical redox ratio in 2D cytokine-stimulated mouse macrophages and 3D mouse monocultures and co-cultures

Time	Coefficient of variation			Squared ranks test
	2D culture			
	M0	M(IFN-γ)	M(IL4/IL13)	Test Statistic
24 hours	0.786	1.05	1.23	-4.512 (*)
48 hours	0.963	0.892	1.08	-78.823 (*)
72 hours	1.04	1.11	1.06	-78.609 (*)
	3D culture			
	Monoculture		Co-culture	
24 hours	0.241		0.357	25.654 (*)
48 hours	0.275		0.385	8.997 (*)
72 hours	0.249		0.339	29.400 (*)

(*) **p <0.05**